JB
Journals.ASM.org

AglS, a Novel Component of the *Haloferax volcanii* N-Glycosylation Pathway, Is a Dolichol Phosphate-Mannose Mannosyltransferase

Chen Cohen-Rosenzweig, Sophie Yurist-Doutsch,* and Jerry Eichler

Department of Life Sciences, Ben Gurion University of the Negev, Beersheva, Israel

In *Haloferax volcanii*, a series of Agl proteins mediates protein N-glycosylation. The genes encoding all but one of the Agl proteins are sequestered into a single gene island. The same region of the genome includes sequences also suspected but not yet verified as serving N-glycosylation roles, such as *HVO_1526*. In the following, HVO_1526, renamed AglS, is shown to be necessary for the addition of the final mannose subunit of the pentasaccharide N-linked to the surface (S)-layer glycoprotein, a convenient reporter of N-glycosylation in *Hfx. volcanii*. Relying on bioinformatics, topological analysis, gene deletion, mass spectrometry, and biochemical assays, AglS was shown to act as a dolichol phosphate-mannose mannosyltransferase, mediating the transfer of mannose from dolichol phosphate to the tetrasaccharide corresponding to the first four subunits of the pentasaccharide N-linked to the S-layer glycoprotein.

Although the ability of *Archaea* to perform protein N-glycosylation was first reported in 1976 (22), only recently have efforts begun to focus on delineating the pathways involved in the archaeal version of this universal posttranslational modification. In the halophile *Haloferax volcanii* (*Hfx. volcanii*), a series of *agl* (*a*rchaeal *gl*ycosylation) genes encode proteins involved in the assembly and attachment of a pentasaccharide to select Asn residues of the surface (S)-layer glycoprotein (7) and, as recently shown, of archaellins, the building blocks of the archaellum (the archaeal flagellum) (15, 30). Acting at the cytoplasmic face of the plasma membrane, AglJ, AglG, AglI, and AglE sequentially add the first four pentasaccharide residues (i.e., a hexose, two hexuronic acids, and the methyl ester of a hexuronic acid) onto a common dolichol phosphate (DolP) carrier, while AglD adds the final pentasaccharide residue, mannose, to a distinct DolP (2, 3, 11, 16, 21, 24, 32). In addition, N-glycosylation roles have been assigned to AglF, a glucose-1-phosphate uridyltransferase (33), AglM, a UDP-glucose dehydrogenase (33), and AglP, a methyltransferase (21). Once assembled, the lipid-charged glycans are translocated across the membrane by an unknown mechanism although AglR is apparently involved in the process (17). In a reaction requiring the oligosaccharyltransferase, AglB (2), the translocated tetrasaccharide and its precursors are delivered from DolP to select Asn residues of the S-layer glycoprotein. Finally, the terminal pentasaccharide residue, mannose, is transferred from its "flipped" DolP carrier to the protein-bound tetrasaccharide (15). Failure to add this final mannose to the S-layer glycoprotein slows *Hfx. volcanii* growth under select conditions, modifies S-layer architecture and stability, and renders the cells nonmotile (2, 30).

Apart from AglD, all of the currently known components of the *Hfx. volcanii* N-glycosylation pathway are encoded by sequences sequestered to a common gene island (31). However, in addition to containing genes of known function, the *agl* gene cluster also includes several sequences whose contribution to N-glycosylation remains to be defined. *HVO_1526* represents one such sequence. Previous studies addressing the open reading frames (ORFs) comprising the *agl* gene cluster demonstrated that *HVO_1526* is transcribed (31). The same is true of the region separating this sequence from *HVO_1527*, corresponding to *aglF*, a known component of the *Hfx. volcanii* N-glycosylation pathway (32), pointing to cotranscription of the two sequences. Still, the function of HVO_1526 and its contribution to N-glycosylation remain elusive.

In the present study, a combination of gene deletion, mass spectrometry, bioinformatics, and biochemical approaches was employed to show that HVO_1526, renamed AglS, catalyzes the transfer of mannose from DolP-mannose to the protein-bound glycan comprising the first four subunits of the N-linked pentasaccharide attached to the *Hfx. volcanii* S-layer glycoprotein.

MATERIALS AND METHODS

Strains and growth conditions. *Hfx. volcanii* WR536 (H53) parent strain cells (4) were grown in medium containing 3.4 M NaCl, 0.15 M $MgSO_4$, 1 mM $MnCl_2$, 4 mM KCl, 3 mM $CaCl_2$, 0.3% (wt/vol) yeast extract, 0.5% (wt/vol) tryptone, and 50 mM Tris-HCl, pH 7.2, at 42°C (23).

Subcellular fractionation. *Hfx. volcanii* cells (1 ml) were broken by sonication (2 s on and 1 s off for 90 s; 25% output; Misonix XL2020 ultrasonicator). Unbroken cells were pelleted in a microcentrifuge (9,000 × *g* for 10 min at 4°C), and the resulting supernatant was centrifuged in an ultracentrifuge (240,000 × *g* for 12 min at 4°C) (Sorvall M120). While the resulting supernatant was directly precipitated in 15% (wt/vol) trichloroacetic acid, the pelleted membrane fraction was resuspended in 200 μl of distilled water and then precipitated in 15% (wt/vol) trichloroacetic acid. Proteins were electrotransferred from SDS-PAGE gels to nitrocellulose membranes (0.45-μm pore size; Schleicher & Schuell, Dassel, Germany) and incubated with polyclonal rabbit anti-cellulose-binding domain (CBD) antibodies (1:10,000 dilution) (a gift from Ed Bayer, Weizmann Institute of Science) or anti-SRP54 antibodies (29). Horseradish peroxidase-conjugated goat anti-rabbit antibodies (Bio-Rad), serving as secondary antibodies, were used at a 1:2,500 dilution. Antibody binding was detected using ECL Western blotting detection reagent (Amersham, Buckinghamshire, United Kingdom). The distribu-

Received 12 September 2012 **Accepted** 10 October 2012

Published ahead of print 19 October 2012

Address correspondence to Jerry Eichler, jeichler@bgu.ac.il.

* Present address: Sophie Yurist-Doutsch, Michael Smith Laboratories, University of British Columbia, Vancouver, British Columbia, Canada.

doi:10.1128/JB.01716-12

tion of the S-layer glycoprotein was determined by Coomassie staining of the cytosolic and membrane protein pools in SDS-PAGE gels.

Generation of CBD- and polyhistidine-tagged HVO_1526. To generate a plasmid encoding N-terminally *Clostridium thermocellum* CBD-tagged HVO_1526 (CBD-HVO_1526), the *HVO_1526* gene was PCR amplified using primers (forward primer, GGG**CATATG**ACAATAGTTAAAAAAGTGGC; reverse primer, CCC**GGTACC**TTAATCATTTTGTCTGCGAC) designed to introduce NdeI and KpnI restriction sites (in boldface in the sequences) at the start and end of the gene, respectively. The amplified fragment was digested with NdeI and KpnI and ligated into plasmid pWL-CBD (14), previously digested with the same restriction enzymes, to produce plasmid pWL-CBD-HVO_1526. Plasmid pWL-CBD-HVO_1526 was introduced into *Hfx. volcanii* parent strain cells.

To generate a plasmid encoding C-terminally polyhistidine-tagged HVO_1526 (His-HVO_1526), *HVO_1526* was PCR amplified using primers (forward primer, **GGGCAT**ATGAAACGATTAGCAAAAGCAGC; reverse primer, **CCCCTCGAG**AGGTAACCTCCATTTTCCACA) designed to introduce NdeI and XhoI restriction sites (in boldface in the primer sequences) at the start and end of the gene, respectively. The amplified fragment was inserted into the pET24 plasmid (Novogen) so as to introduce DNA encoding a polyhistidine tag, cleaved with the same enzymes. The tag-bearing fragment was then excised upon digestion with NdeI and BlpI and ligated into plasmid pJAM-202 (25), previously digested with the same restriction enzymes, to produce plasmid pHis-HVO_1526. Plasmid pHis-HVO_1526 was then introduced into *Hfx. volcanii* Δ*HVO_1526* cells.

Deletion of *HVO_1526*. Deletion of *Hfx. volcanii HVO_1526* was achieved using a previously described approach (1, 4). To amplify approximately 500-bp-long regions flanking the coding sequence of *HVO_1526*, the aglS-5′upfor (GGGGGTACC**TGGGGAAGGACGTTGAGAAT**; genomic sequence is in boldface letters) and aglS-5′uprev (CCCAAGCTT**CATACTTGGCTCTCTATTAG**) primers, directed against the upstream flanking region, and the aglS-3′downfor (GGGGGATCC**TAACCGCAGGACACCAACCC**) and aglS-3′downrev (CCCTCTAGA**TTGGCGTTGAAGATGTTGTC**) primers, directed against the downstream flanking region, were employed. KpnI and HindIII sites were introduced using the aglS-5′upfor and aglS-5′uprev primers, respectively, while BamHI and XbaI sites were introduced using the aglS-3′downfor and aglS-3′downrev primers, respectively. To confirm deletion of *HVO_1526* at the DNA level, PCR amplification was performed using forward primers directed against either an internal region of *HVO_1526* (aglS-for; ATGAAACGATTAGCAAAAGCAGCATTC) or *trpA* (CCCGAATTC**TTATGTGCGTTCCGGATGCG**) together with a reverse primer against a region downstream of *HVO_1526* (aglS-5′downrev; TCAAGGTAACCTCCATTTTCCACAC), yielding primer pairs a and b.

To confirm deletion of *HVO_1526* at the RNA level, reverse transcription-PCR (RT-PCR) was performed as described previously (1). RNA isolation was carried out using an Easy-Spin RNA extraction kit (Intron Biotechnology, Kyungki-Do, South Korea), according to the manufacturer's instructions. RNA concentration was determined spectrophotometrically. After contaminating DNA was eliminated with a DNAFree kit (Ambion, Austin TX), single-stranded cDNA was prepared for each sequence from the corresponding RNA (2 μg) using random hexamers (150 ng) in a SuperScript III First-Strand Synthesis System for RT-PCR (Invitrogen, Carlsbad CA). The single-stranded cDNA was then used as the PCR template in a reaction mixture containing the appropriate forward (ATGAAACGATTAGCAAAAGCAGCATTC) and reverse (TCAAGGTAACCTCCATTTTCCACAC) primers. cDNA amplification was monitored by electrophoresis in 1% agarose gels. The sequences of the PCR products were determined to confirm their identity. In control experiments, PCR amplification was performed on total RNA prior to cDNA preparation to exclude any contribution from contaminating DNA or in the absence of nucleic acids.

LC-ESI MS. Liquid chromatography-electrospray ionization mass spectrometry (LC-ESI MS) analysis of the *Hfx. volcanii* S-layer glycoprotein was performed as previously described (6).

***In vitro* AglS assay.** CBD-AglS was purified as described by Irihimovitch et al. (14). Briefly, transformed cells (1 ml) were centrifuged (3,000 × *g* for 3 min at room temperature [RT]) and resuspended in 1 ml of lysis buffer (1% Triton X-100 [vol/vol], 1.8 M NaCl, 50 mM Tris-HCl, pH 7.2) containing 1 mM phenylmethylsulfonyl fluoride (PMSF). The mixtures were rocked (10 min at RT), after which time 50 μl of a 10% (wt/vol) solution of cellulose beads was added. After 20 min of rocking at RT, the suspension was centrifuged (3,000 × *g* for 3 min at RT), the supernatant was discarded, and the cellulose pellet was washed with 2 M NaCl, 50 mM Tris-HCl, pH 7.2. This washing procedure was repeated twice. Fifty microliters of cellulose-bound CBD-AglS slurry was combined with 50 μl of membranes prepared from Δ*aglS* cells and 200 μl of buffer (2 M NaCl, 50 mM Tris-HCl, pH 7.2). The membranes were prepared from 5 ml of cells grown to exponential phase as performed for subcellular fractionation, described above. After 0 to 3 h of incubation at 42°C, the CBD-AglS-bearing cellulose beads were collected by centrifugation (3,000 rpm for 5 min in a microcentrifuge), and the supernatant, containing the membrane fragments, was precipitated with 7.5% trichloroacetic acid on ice. The precipitated proteins were rinsed with ice-cold acetone and subjected to 10% SDS-PAGE. Coomassie-stained bands corresponding to the S-layer glycoprotein were excised and analyzed by LC-ESI MS.

RESULTS

***Hfx. volcanii HVO_1526* encodes a multispanning membrane protein.** To determine whether *HVO_1526* indeed corresponds to a true protein-encoding gene, *Hfx. volcanii* cells were transformed to express HVO_1526 bearing an N-terminal *Clostridium thermocellum* cellulose-binding domain (CBD). The presence of the *C. thermocellum* CBD allows for cellulose-based purification in the hypersaline environment required for *Hfx. volcanii* survival (14). An immunoblot of a total protein extract of parent strain cells and cells transformed to express CBD-HVO_1526 using anti-CBD antibodies revealed the presence of a band of approximately 68 kDa, corresponding to the combined masses of CBD (17,215 Da) and HVO_1526 (50,525 Da), only in the extract of the transformed cells (Fig. 1A).

To determine the localization of HVO_1526, cells expressing CBD-HVO_1526 were subjected to subcellular fractionation. The presence of HVO_1526 in the membrane and cytoplasmic fractions was then tested by immunoblotting using anti-CBD antibodies. Such efforts confirmed the membrane localization of HVO_1526 (Fig. 1B). Control experiments confirmed the cytoplasmic localization of SRP54 (29), reflecting the efficacy of the subcellular fractionation. Next, various topology prediction servers were consulted to define HVO_1526 topology. The TMHMM (http://www.cbs.dtu.dk/services/TMHMM-2.0/), TMpred (http://www.ch.embnet.org/software/TMPRED_form.html), SOSUI (http://bp.nuap.nagoya-u.ac.jp/sosui/), TopPred (http://bioweb.pasteur.fr/seqanal/interfaces/toppred.html), and HMMTOP (http://www.enzim.hu/hmmtop/) servers all agreed that the 457-amino-acid-residue-containing HVO_1526 is a multispanning membrane protein, presenting nine transmembrane domains and a cytoplasmically oriented N terminus, as well as major externally oriented domains between the first two transmembrane domains and in the C-terminal portion of the protein comprising some 50 and 100 residues, respectively. A schematic depiction of the predicted topology of HVO_1526, as determined by the SOSUI server, is offered in Fig. 1C.

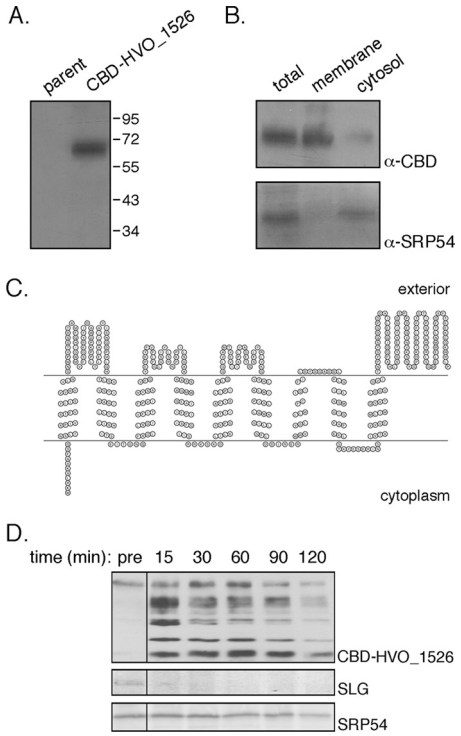

FIG 1 *Hfx. volcanii* HVO_1526 is a membrane protein. (A) Total extracts of *Hfx. volcanii* parent strain cells and cells transformed to express CBD-HVO_1526 were probed with anti-CBD antibodies. The positions of molecular weight markers are indicated on the right. (B) *Hfx. volcanii* cells transformed to express CBD-HVO_1526 were separated into membrane and cytosolic fractions and probed with anti-CBD (α-CBD) and anti-SRP54 (α-SRP54) antibodies, as was a total protein extract. (C) Schematic depiction of the topology of HVO_1526 according to the SOSUI server, drawn using Topo2 software (http://www.sacs.ucsf.edu/TOPO2/). The N terminus is found at the left end of the sequence. (D) *Hfx. volcanii* cells transformed to express CBD-HVO_1526 were challenged with proteinase K (1 mg/ml; 2 h at 55°C). After separation by SDS-PAGE, the S-layer glycoprotein (SLG) was identified by Coomassie staining (middle panel), while CBD-HVO_1526 (upper panel) and SRP54 (lower panel) were identified by immunoblotting using appropriate antibodies. The presence of CBD-HVO_1526 (and derived proteolytic fragments), the S-layer glycoprotein, and SRP54 was assessed before the addition of proteinase K (pre) and 15, 30, 60, 90, and 120 min after proteinase K addition.

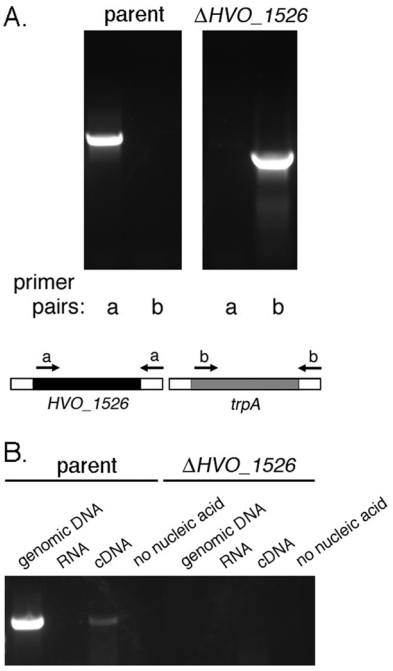

FIG 2 *Hfx. volcanii HVO_1526* is not an essential gene. (A) The DNA from *Hfx. volcanii* parent strain cells (left panel) and from cells deleted of *HVO_1526* (right panel) served as the template in PCR amplifications using primers directed against *HVO_1526* (primer pair a) or *trpA* (primer pair b). The binding positions of each primer pair are schematically depicted. (B) RT-PCR was performed using primers directed against *HVO_1526* together with genomic DNA, RNA, or cDNA prepared from *Hfx. volcanii* parent strain cells (left) and from cells deleted of *HVO_1526* (right) (or no nucleic acid) as the template.

To experimentally test these predictions, cells expressing CBD-HVO_1526 were challenged with proteinase K. Immunoblot analysis of aliquots removed before and at successive intervals after addition of the protease was performed using anti-CBD antibodies (Fig. 1D). Before proteinase K addition, the antibodies identified a single band, corresponding to CBD-HVO_1526. After 15 min of proteolysis, additional faster-migrating bands appeared, corresponding to the CBD N-terminally fused to HVO_1526 fragments of different lengths. With continued proteolytic digestion, the fastest-migrating band became the most intensely stained species. Protection of the immunolabeled CBD moiety fused to the HVO_1526 N terminus from externally added protease points to this segment of the chimera as being sequestered within the cell, in agreement with the server-based topology predictions. Indeed, when membrane integrity was disrupted upon addition of 1% Triton X-100, the CBD moiety was readily digested by added proteinase K (data not shown). Finally, to confirm that the added protease did not compromise cell integrity, levels of the S-layer glycoprotein, a marker of the external surface of the cell (28), and of SRP54, a marker of the intracellular compartment (29), were assessed. Whereas the former was fully digested within 30 min, SRP54 could be detected for the duration of the experiment, with only limited digestion being detected after 2 h (Fig. 1D).

The N-linked glycan decorating the S-layer glycoprotein in Δ*HVO_1526* cells lacks the final mannose subunit. To determine whether HVO_1526 participates in N-glycosylation, *Hfx. volcanii* cells lacking the encoding gene were generated according to the method of Allers et al. (4), as described in Materials and Methods. Briefly, *HVO_1526* was replaced by *trpA*, encoding tryptophan synthase, in an *Hfx. volcanii* strain auxotrophic for tryptophan. To confirm replacement of *HVO_1526* by *trpA* at the DNA level, PCR was performed using primers directed at either *HVO_1526* (primer pair a) or *trpA* (primer pair b). *HVO_1526* was detected solely in the parent strain, whereas only the deletion strain contained *trpA* (Fig. 2A). To confirm deletion of *HVO_1526* at the RNA level, RT-PCR was performed. Such experiments revealed that while a PCR product corresponding to *HVO_1526* was generated when genomic DNA or cDNA prepared from parent strain cells served as the template, no such products were generated when the same templates generated from Δ*HVO_1526* cells were used (Fig. 2B).

To assess the importance of HVO_1526 to N-glycosylation, parent and Δ*HVO_1526* strain S-layer glycoprotein-derived tryptic peptides, including the N-terminal ^{1}ERGNLDADSESFNK^{14} fragment that contains the glycosylated Asn-13 residue (2), were examined by liquid chromatography-electrospray ionization

mass spectrometry (LC-ESI MS). Such analysis revealed the presence of peaks corresponding to the Asn-13-containing S-layer glycoprotein-derived peptide obtained from the parent strain modified by a pentasaccharide (*m/z* 1,224.48) (Fig. 3A, left-most column, top panel) comprising a hexose, two hexuronic acids, a methyl ester of hexuronic acid, and a terminal mannose residue (2, 12, 21). In addition, peaks corresponding to the same peptide modified by the precursor tetra- (*m/z* 1,143.45), tri- (*m/z* 1,048.42), di- (*m/z* 960.41), and monosaccharides (*m/z* 872.38) were also observed (Fig. 3A, left-most column, middle and bottom panels, and third column, top and bottom panels, respectively). In contrast, cells lacking HVO_1526 did not present peaks corresponding to the pentasaccharide-modified Asn-13-containing peptide (Fig. 3A, second column, top panel) even though peaks reflecting the same peptide modified by the precursor tetra- (*m/z* 1,143.95), tri- (*m/z* 1,048.42), di- (*m/z* 960.41), and monosaccharide (*m/z* 872.39) were detected (Fig. 3A, second column, middle and bottom panels, and right-most column, top and bottom panels, respectively). When, however, cells of the deletion strain were transformed to express a polyhistidine-tagged version of HVO_1526, it was observed that the Asn-13-containing S-layer glycoprotein-derived peptide was once again modified by the complete pentasaccharide (Fig. 3B). In each figure panel, $[M+2H]^{2+}$ ion peaks are shown.

Given the contribution of HVO_1526 to *Hfx. volcanii* N-glycosylation, the protein was renamed AglS, according to the nomenclature for archaeal N-glycosylation pathway components first proposed by Chaban et al. (10).

Bioinformatics predictions of AglS function. As a first step toward more precisely defining AglS function, the sequence of the protein was used as a query in a BLAST search (http://blast.ncbi.nlm.nih.gov/Blast.cgi). Such efforts identified only three homologues showing substantial similarity to AglS, namely, *Haloarcula hispanica* (*Har. hispanica*) HAH_2530 (E value of 6e−54; 92% coverage, 32% identity), *Haloarcula marismortui* (*Har. marismortui*) rrnAC2035 (E value of 2e−52; 89% coverage, 32% identity) and *Haloterrigena turkmenica* (*Htg. turkmenica*) Htur_2596 (E value of 2e−47; 91% coverage, 27% identity). Like AglS, each of these haloarchaeal proteins is currently annotated as a hypothetical protein with no predicted function. Indeed, neither InterProScan (http://www.ebi.ac.uk/Tools/InterProScan/) nor Conserved Domain Database (http://www.ncbi.nlm.nih.gov/Structure/cdd/cdd.shtml) searches recognized known domains in AglS or the homologous haloarchaeal sequences.

Next, AglS served as a query in a psiBLAST search against archaeal genome sequences available at the NCBI BLAST site (http://blast.ncbi.nlm.nih.gov/Blast.cgi). After five iterations, numerous putative AglS homologues were detected. Of those showing query coverage of ≥90%, the three haloarchaeal sequences listed above were identified, as was *Htg. turkmenica* Htur_3525 (E value of 1e−40; 96% coverage, 24% identity), a hypothetical protein with no predicted function. Other archaeal sequences were also identified as AglS homologues in the psiBLAST search, presenting E values as low as 6e−42. While many of these predicted homologues are annotated as arginyl-tRNA synthases or oligosaccharide transferase STT3 subunits (equivalent to *Hfx. volcanii* AglB [2]), several are annotated as DolP-mannose-protein mannosyltransferases (Carbohydrate-Active Enzymes [CAZy] database [http://www.cazy.org/Home.html]) glycosyltransferase family 39; EC 2.4.1.109), namely, enzymes responsible for transferring mannose residues attached to DolP to protein targets in the endoplasmic reticulum (ER) during O-glycosylation in *Saccharomyces cerevisiae* (27). These include *Halobacterium* sp. DL1 locus ZP_09028934 (E value of 5e−24; 90% coverage), *Methanoculleus marisnigri* Memar_0728 (E value of 2e−20; 62% coverage), *Thermococcus litoralis* OCC_09791 (E value of 2e−19; 76% coverage), *Haladaptatus paucihalophilus* ZOD2009_13791 (E value of 3e−19; 85% coverage), *Haladaptatus paucihalophilus* ZOD2009_20562 (E value of 4e−19; 83% coverage), *Pyrococcus abyssi* PAB0056 (E value of 3e−17; 73% coverage), *Methanosarcina barkeri* Mbar_A0497 (E value of 3e−17; 76% coverage) and *Methanoplanus petrolearius* Mpet_0696 (E value of 1e−16; 58% coverage). When the CAZy database was scanned (May 2012) for archaeal enzymes assigned to glycosyltransferase family 39, three crenarchaeotal sequences were identified (*Pyrococcus abyssi* PAB0056, *Pyrobaculum* sp. 1860 locus tag P186_0005 [gi 356640796], and "*Candidatus* Caldiarchaeum subterraneum" HGMM_F55E04C20). Of these, *Pyrococcus abyssi* PAB0056 was identified in the psiBLAST search described above as a homologue of AglS.

Based on these bioinformatics observations, it was hypothesized that AglS acts as a DolP-mannose mannosyltransferase.

AglS functions as a DolP-mannose mannosyltransferase. To begin testing whether or not AglS serves to transfer mannose from DolP-mannose to the four-member N-linked pentasaccharide precursor bound to the S-layer glycoprotein, efforts were initially directed at obtaining the purified protein. Accordingly, cellulose-based chromatography captured a CBD-AglS-sized band from a total cell extract of *Hfx. volcanii* cells transformed to express this chimera but not from an extract of nontransformed cells (Fig. 4A, upper panel). The recognition of this band by anti-CBD antibodies both in the transformed cell extract and following cellulose-based purification confirmed its identity as CBD-AglS (Fig. 4A, lower panel).

With cellulose-purified CBD-AglS in hand, an *in vitro* assay was developed. In the assay (schematically depicted in Fig. 4B), cellulose-bound CBD-AglS was incubated with membrane fragments prepared from Δ*aglS* cells. AglS-mediated transfer of mannose from DolP-mannose to the glycan N-linked to *Hfx. volcanii* S-layer glycoprotein Asn-13 was subsequently assessed by LC-ESI MS. Accordingly, LC-ESI MS revealed that prior to CBD-AglS addition, the precursor tetrasaccharide decorated the S-layer glycoprotein from the mutant strain at this position (Fig. 4C, left column, lower panel) but not the complete pentasaccharide (Fig. 4C, left column, upper panel). When, however, membrane fragments prepared from Δ*aglS* cells were combined with cellulose-bound CBD-AglS, the Asn-13-containing S-layer glycoprotein-derived peptide was now modified by the complete pentasaccharide (Fig. 4C, right column, upper panel). When the same membrane fragments were incubated with cellulose-bound CBD alone, only the N-linked tetrasaccharide was observed. Similarly, only tetrasaccharide-modified S-layer glycoprotein Asn-13 was observed upon incubation of membrane fragments prepared from Δ*aglS* cells with cellulose-bound CBD-SecY, another multiple membrane-spanning *Hfx. volcanii* protein (14). On the other hand, the absence of AglR, thought to translocate DolP-mannose across the plasma membrane (17), did not prevent the ability of CBD-AglS to attach the final mannose of the pentasaccharide decorating S-layer glycoprotein Asn-13. Finally, to confirm that the mannose subunit that was transferred to the protein-bound tet-

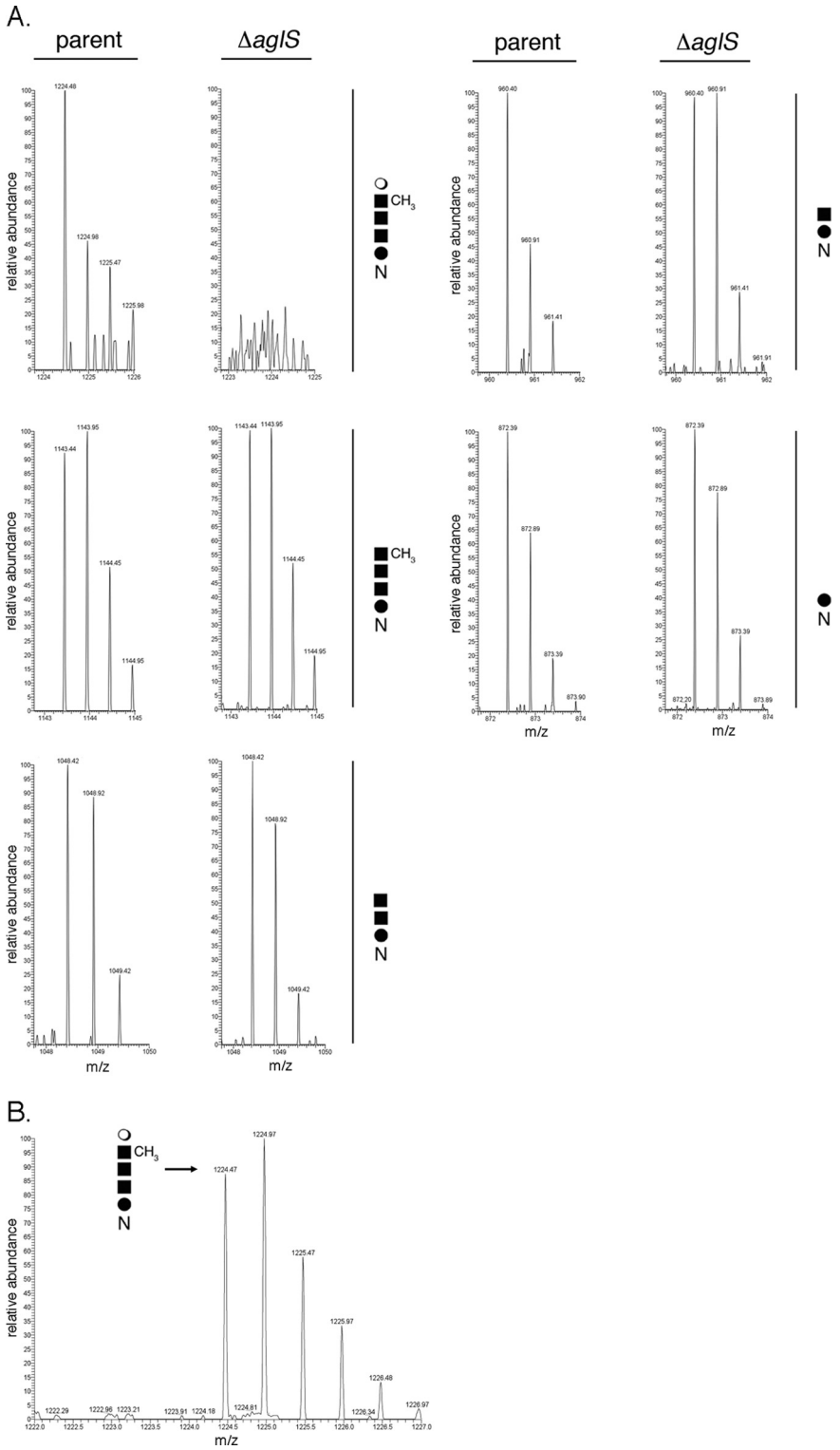

FIG 3 In cells lacking HVO_1526, the final mannose residue of the N-linked glycan decorating the S-layer glycoprotein is absent. (A) LC-ESI MS profile of an S-layer glycoprotein-derived Asn-13-containing peptide generated from *Hfx. volcanii* parent strain cells (left panel of each pair) and from cells deleted of *HVO_1526* (right panel of each pair). The composition of the glycan modifying the peptide in each pair of panels is schematically depicted on the right of each pair. (B) LC-ESI MS profile of an S-layer glycoprotein-derived Asn-13-containing peptide generated from *Hfx. volcanii* cells deleted of *HVO_1526* and transformed to express polyhistidine-tagged HVO_1526. The peak corresponding to the pentasaccharide-modified peptide is indicated, as is a schematic depiction of the pentasaccharide. In each panel of the figure, $[M+2H]^{2+}$ ion peaks are shown.

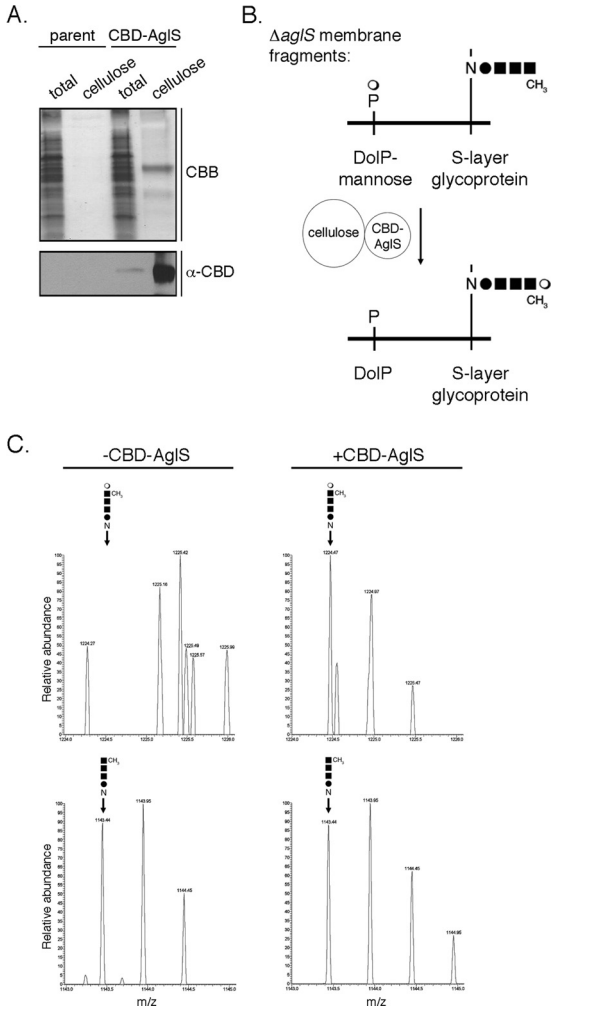

FIG 4 AglS functions as a DolP-mannose mannosyltransferase. (A) Cellulose-based purification of CBD-AglS from protein extracts of *Hfx. volcanii* parent strain cells and of cells transformed to express CBD-AglS was performed. The total protein extract and cellulose-bound proteins from each strain were separated by 10% SDS-PAGE, stained with Coomassie brilliant blue (CBB) and analyzed by immunoblotting using antibodies raised against the CBD moiety (α-CBD). (B) Schematic depiction of the *in vitro* assay of AglS function employed. Membrane fragments prepared from Δ*aglS* cells were combined with cellulose-bound CBD-AglS for 0 to 3 h at 42°C. Aliquots were drawn at 1-h intervals, and LC-ESI MS was performed to determine whether AglS catalyzes the transfer of mannose from DolP-mannose to the glycan corresponding to the first four subunits of the pentasaccharide normally N-linked to the protein, as described in Materials and Methods. (C) LC-ESI MS analysis of an Asn-13-containing S-layer glycoprotein-derived peptide from Δ*aglS* cells before (−CBD-AglS column) and 3 h after (+CBD-AglS column) incubation with cellulose-bound CBD-AglS. In each column, the upper panel presents that region of the LC-ESI MS profile containing pentasaccharide-modified peptide, while the lower panel reflects that region of the profile containing tetrasaccharide-modified peptide. In each panel, the identity and position of the peak in question are indicated. The results are representative of four repeats of the experiment.

rasaccharide via the actions of AglS was, indeed, derived from DolP-mannose, the *in vitro* assay was repeated, this time using cellulose-bound CBD-AglS and membrane fragments prepared from Δ*aglD* cells lacking DolP-mannose (2, 12). As expected, in the absence of DolP-mannose, incubation of a tetrasaccharide-modified S-layer glycoprotein with CBD-AglS did not lead to the appearance of the complete pentasaccharide at Asn-13. These results are summarized in Table 1.

DISCUSSION

In *Hfx. volcanii*, a series of Agl proteins is responsible for the assembly and attachment of a pentasaccharide to select Asn residues of the S-layer glycoprotein and archaellin (7, 30). Although the enzymes catalyzing most of the steps of the Agl pathway have been described, the agents mediating several central steps of the process remain undefined. For example, it remains unclear how mannose, added to DolP on the cytoplasmic face of the plasma membrane (24), finds its way to the tetrasaccharide precursor of the pentasaccharide N-linked to the S-layer glycoprotein on the external surface of the cell (9). The present study shows that AglS is involved in this process.

The attachment of mannose to DolP and subsequently to the N-linked tetrasaccharide requires, at minimum, the sequential activities of a DolP-mannose synthase, a DolP-mannose flippase, and a DolP-mannose mannosyltransferase. Given the absence of the final mannose subunit on the glycan N-linked to the S-layer glycoprotein in Δ*aglS* cells, it would seem that AglS assumes one of these roles. Earlier studies have shown AglD to be a DolP-mannose synthase, responsible for charging DolP with the mannose subsequently added to the S-layer glycoprotein-bound tetrasaccharide (2, 8, 9, 12). Accordingly, the presence of AglS could not compensate for the absence of AglD in the *in vitro* assay developed here. Instead, the results of *in silico*, *in vivo*, and *in vitro* experiments together support the assignment of AglS as a DolP-mannose mannosyltransferase, responsible for delivering mannose from its dedicated DolP carrier to the N-linked tetrasaccharide decorating the S-layer glycoprotein. At the same time, several lines of evidence argue against AglS acting as a DolP-mannose flippase. First, bioinformatics fails to identify domains in AglS shared by other predicted lipid-linked oligosaccharide flippases, such as Rft1, PglK, or Wzx. Second, in the *in vitro* assay developed here, DolP-mannose flippase activity is not required since the topology of the added membrane fragments is not preserved. Yet addition of the final mannose of the N-linked glycan did not occur in the absence of AglS. Moreover, evidence supporting a DolP-mannose flippase role for AglR has been recently provided (17). Indeed, successful addition of the final mannose of the N-linked pentasaccharide was realized in the *in vitro* assay using membranes prepared from Δ*aglR* cells. While the transfer of mannose from DolP-mannose to the S-layer glycoprotein-bound tetrasaccharide was not directly shown to transpire on the external surface of the cell in this study, several observations point this to indeed being the case. The predicted existence of large externally oriented soluble domains in AglS argues that the protein acts on DolP-mannose only after the sugar-charged lipid carrier has been translocated across

TABLE 1 *In vitro* assay of AglS activity

Added protein	Source of membrane fragments	S-layer glycoprotein Asn-13-linked glycan
CBD-AglS	*Hfx. volcanii* Δ*aglS*	Pentasaccharide
CBD	*Hfx. volcanii* Δ*aglS*	Tetrasaccharide
CBD-SecY	*Hfx. volcanii* Δ*aglS*	Tetrasaccharide
CBD-AglS	*Hfx. volcanii* Δ*aglD*	Tetrasaccharide
CBD-AglS	*Hfx. volcanii* Δ*aglR*	Pentasaccharide

the plasma membrane. In addition, earlier studies have provided evidence to show that the oligosaccharyltransferase, AglB, responsible for adding the tetrasaccharide precursor of N-linked pentasaccharide to the S-layer glycoprotein (2), catalyzed this reaction on the external surface of the cell (18). As such, the subsequent transfer of mannose from DolP-mannose to the N-linked tetrasaccharide would also transpire on the outer cell surface.

When archaeal homologues of AglS were sought, these were detected only in *Har. hispanica*, *Htg. turkmenica*, and *Har. marismortui*. Presently, nothing is known regarding the pathway or, indeed, the existence of N-glycosylation in either *Har. hispanica* or *Htg. turkmenica*. In contrast, it has been shown that the *Har. marismortui* S-layer glycoprotein is N-glycosylated by a similar if not the same pentasaccharide (i.e., hexose-hexuronic acid-hexuronic acid-methyl ester of hexuronic acid-mannose) as N-linked to the *Hfx. volcanii* S-layer glycoprotein (8). However, unlike what occurs in *Hfx. volcanii*, where the final pentasaccharide subunit, mannose, is added to the glycan comprising the first four subunits of the pentasaccharide already N-linked to the S-layer glycoprotein, the intact pentasaccharide is delivered to the S-layer glycoprotein from a single common DolP carrier in *Har. marismortui* (8, 9). Nonetheless, DolP-mannose is detected as an intermediate in both species (8). As such, it is conceivable that the *Har. marismortui* homologue of AglS transfers mannose from its DolP carrier to the DolP-bound tetrasaccharide prior to delivery of the complete pentasaccharide to the S-layer glycoprotein in this organism.

Bioinformatics served to detect homology between AglS and DolP-mannose-protein *O*-mannosyltransferases (27). However, closer comparison of AglS and DolP-mannose-protein *O*-mannosyltransferases, all belonging to CAZy glycosyltransferase family 39, revealed major differences between the two. In terms of topology, AglS is predicted to possess nine transmembrane domains, as opposed to the seven membrane-spanning domains assigned to the protein *O*-mannosyltransferases (19, 26). Moreover, the positions of the major extracytoplasmic loops in each protein are not the same. More importantly, AglS does not include the highly conserved Asp-Glu motif found in the first extracytosolic loop and involved in the catalytic activity of the O-glycosylation-related DolP-mannose-protein mannosyltransferases or other important residues conserved in known or predicted protein mannosyltransferases from all three domains of life (including from the *Archaea* "*Candidatus* Caldiarchaeum subterraneum," and *Archaeoglobus profundus*) (20) although such a motif is detected in the C-terminal extracytosolic region of AglS. For instance, the invariant Arg residue found in transmembrane domain 2 of the protein *O*-mannosyltransferases and also deemed crucial for enzyme activity (11) is not detected in AglS. As such, it is not clear that AglS belongs to CAZy glycosyltransferase family 39, as do all known DolP-mannose-protein *O*-mannosyltransferases. Rather, AglS is functionally reminiscent of Alg3 (belonging to CAZy glycosyltransferase family 58), Alg9 and Alg12 (both belonging to CAZy glycosyltransferase family 22), namely, DolP α-mannosyltransferases that catalyze the delivery of mannose subunits from DolP-mannose to more complex glycans in the eukaryal N-glycosylation process. Specifically, Alg3, Alg9, and Alg12 sequentially transfer mannose subunits from DolP-mannose assembled on the cytoplasmic face of the ER membrane and flipped to face the ER lumen to glycans based on dolichol pyrophosphate (DolPP)-bound *N*-acetylglucosamine$_2$mannose$_5$, the core glycan of N-linked oligosaccharides in yeast and higher organisms (5, 13). As such and as previously proposed (30), the *Hfx. volcanii* N-glycosylation pathway is reminiscent of its eukaryal counterpart in that in both cases soluble nucleotide-activated sugars are sequentially added to a common phosphodolichol carrier on the cytoplasmic face of a membrane. Once the glycan-charged lipid (tetrasaccharide-charged DolP in *Hfx. volcanii* and heptasaccharide-charged DolPP in *Eukarya*) is assembled, it is translocated across that membrane, at which point the glycan is subjected to further modification via the attachment of additional sugar subunits transferred from flipped monosaccharide-charged DolP, either when still lipid linked (as in *Eukarya*) or following transfer to the target protein (as in *Hfx. volcanii*). Still, the fact that no archaeal members of CAZy glycosyltransferase family 58 (such as Alg3) or 22 (such as Alg9 and Alg12) are known serves as a reminder that N-glycosylation processes in *Eukarya* and *Archaea* are distinct.

As more is learned of archaeal (and bacterial) protein glycosylation, further insight into the origins of this universal post-translational modification will be provided.

ACKNOWLEDGMENTS

J.E. is supported by grants from the Israel Science Foundation (8/11) and the U.S. Army Research Office (W911NF-11-1-520). S.Y.-D. held a Negev-Faran Associates Scholarship.

REFERENCES

1. **Abu-Qarn M, Eichler J.** 2006. Protein N-glycosylation in *Archaea*: defining *Haloferax volcanii* genes involved in S-layer glycoprotein glycosylation. Mol. Microbiol. **61**:511–525.
2. **Abu-Qarn M, et al.** 2007. *Haloferax volcanii* AglB and AglD are involved in N-glycosylation of the S-layer glycoprotein and proper assembly of the surface layer. J. Mol. Biol. **374**:1224–1236.
3. **Abu-Qarn M, et al.** 2008. Identification of AglE, a second glycosyltransferase involved in N-glycosylation of the *Haloferax volcanii* S-layer glycoprotein. J. Bacteriol. **190**:3140–3146.
4. **Allers T, Ngo HP, Mevarech M, Lloyd RG.** 2004. Development of additional selectable markers for the halophilic archaeon *Haloferax volcanii* based on the *leuB* and *trpA* genes. Appl. Environ. Microbiol. **70**:943–953.
5. **Burda P, Aebi M.** 1999. The dolichol pathway of N-linked glycosylation. Biochim. Biophys. Acta **1426**:239–257.
6. **Calo D, Eilam Y, Lichtenstein RG, Eichler J.** 2010. Towards glycoengineering in *Archaea*: replacing *Haloferax volcanii* AglD with homologous glycosyltransferases from other halophilic archaea. Appl. Environ. Microbiol. **76**:5684–5692.
7. **Calo D, Kaminski L, Eichler J.** 2010. Protein glycosylation in *Archaea*: sweet and extreme. Glycobiology **20**:1065–1079.
8. **Calo D, Guan Z, Eichler J.** 2011. Glyco-engineering in *Archaea*: differential N-glycosylation of the S-layer glycoprotein in a transformed *Haloferax volcanii* strain. Microb. Biotechnol. **4**:461–470.
9. **Calo D, Guan Z, Naparstek S, Eichler J.** 2011. Different routes to the same ending: comparing the N-glycosylation processes of *Haloferax volcanii* and *Haloarcula marismortui*, two halophilic archaea from the Dead Sea. Mol. Microbiol. **81**:1166–1177.
10. **Chaban B, Voisin S, Kelly J, Logan SM, Jarrell KF.** 2006. Identification of genes involved in the biosynthesis and attachment of *Methanococcus voltae* N-linked glycans: insight into N-linked glycosylation pathways in *Archaea*. Mol. Microbiol. **61**:259–268.
11. **Girrbach V, Zeller T, Preismeier M, Strahl S.** 2000. Structure-function analysis of the dolichyl phosphate-mannose:protein O-mannosyltransferase Scpmt1p. J. Biol. Chem. **275**:19288–19296.
12. **Guan Z, Naparstek S, Kaminski L, Konrad Z, Eichler J.** 2010. Distinct glycan-charged phosphodolichol carriers are required for the assembly of the pentasaccharide N-linked to the *Haloferax volcanii* S-layer glycoprotein. Mol. Microbiol. **78**:1294–1303.

13. **Helenius A, Aebi M.** 2004. Roles of N-linked glycans in the endoplasmic reticulum. Annu. Rev. Biochem. **73**:1019–1049.
14. **Irihimovitch V, Ring G, Elkayam T, Konrad Z, Eichler J.** 2003. Isolation of fusion proteins containing SecY and SecE, components of the protein translocation complex from the halophilic archaeon *Haloferax volcanii*. Extremophiles **7**:71–77.
15. **Jarrell KF, Albers SV.** 2012. The archaellum: an old motility structure with a new name. Trends Microbiol. **20**:307–312.
16. **Kaminski L, et al.** 2010. AglJ adds the first sugar of the N-linked pentasaccharide decorating the *Haloferax volcanii* S-layer glycoprotein. J. Bacteriol. **192**:5572–5579.
17. **Kaminski L, Guan Z, Abu-Qarn M, Konrad Z, Eichler J.** 2012. AglR is required for addition of the final mannose residue of the N-linked glycan decorating the *Haloferax volcanii* S-layer glycoprotein. Biochim. Biophys. Acta **1820**:1664–1670.
18. **Lechner J, Wieland F, Sumper M.** 1985. Biosynthesis of sulfated saccharides N-glycosidically linked to the protein via glucose. Purification and identification of sulfated dolichyl monophosphoryl tetrasaccharides from halobacteria. J. Biol. Chem. **260**:860–866.
19. **Lommel M, Strahl S.** 2009. Protein O-mannosylation: conserved from bacteria to humans. Glycobiology **19**:816–828.
20. **Lommel M, Schott A, Jank T, Hofmann V, Strahl S.** 2011. A conserved acidic motif is crucial for enzymatic activity of protein O-methyltransferases. J. Biol. Chem. **286**:39768–39775.
21. **Magidovich H, et al.** 2010. AglP is a cytoplasmic S-adenosyl-L-methionine-dependent methyltransferase that participates in the N-glycosylation pathway of *Haloferax volcanii*. Mol. Microbiol. **76**:190–199.
22. **Mescher MF, Strominger JL.** 1976. Purification and characterization of a prokaryotic glycoprotein from the cell envelope of *Halobacterium salinarium*. J. Biol. Chem. **251**:2005–2014.
23. **Mevarech M, Werczberger R.** 1985. Genetic transfer in. *Halobacterium volcanii*. J. Bacteriol. **162**:461–462.
24. **Plavner N, Eichler J.** 2008. Defining the topology of the N-glycosylation pathway in the halophilic archaeon. *Haloferax volcanii*. J. Bacteriol. **190**: 8045–8052.
25. **Reuter CJ, Kaczowka SJ, Maupin-Furlow JA.** 2004. Differential regulation of the PanA and PanB proteasome-activating nucleotidase and 20S proteasomal proteins of the haloarchaeon *Haloferax volcanii*. J. Bacteriol. **186**:7763–7772.
26. **Strahl-Bolsinger S, Scheinost A.** 1999. Transmembrane topology of pmt1p, a member of an evolutionarily conserved family of protein O-mannosyltransferases. J. Biol. Chem. **274**:9068–9075.
27. **Strahl-Bolsinger S, Gentzsch M, Tanner W.** 1999. Protein O-mannosylation. Biochim. Biophys. Acta **1426**:297–307.
28. **Sumper M, Berg E, Mengele R, Strobel I.** 1990. Primary structure and glycosylation of the S-layer protein of *Haloferax volcanii*. J. Bacteriol. **172**: 7111–7118.
29. **Tozik I, Huang Q, Zwieb C, Eichler J.** 2002. Reconstitution of the signal recognition particle of the halophilic archaeon *Haloferax volcanii*. Nucleic Acids Res. **30**:4166–4175.
30. **Tripepi M, et al.** 2012. N-Glycosylation of *Haloferax volcanii* flagellins requires known Agl proteins and is essential for biosynthesis of stable flagella. J. Bacteriol. **194**:4876–4887.
31. **Yurist-Doutsch S, Eichler J.** 2009. Manual annotation, transcriptional analysis and protein expression studies reveal novel genes in the *agl* cluster responsible for N-glycosylation in the halophilic archaeon *Haloferax volcanii*. J. Bacteriol. **191**:3068–3075.
32. **Yurist-Doutsch S, et al.** 2008. *aglF*, aglG and *aglI*, novel members of a gene cluster involved in the N-glycosylation of the *Haloferax volcanii* S-layer glycoprotein. Mol. Microbiol. **69**:1234–1245.
33. **Yurist-Doutsch S, et al.** 2010. N-glycosylation in *Archaea*: on the coordinated actions of *Haloferax volcanii* AglF and AglM. Mol. Microbiol. **75**:1047–1058.